


A Proteolytic Complex Targets Multiple Cell Wall Hydrolases in *Pseudomonas aeruginosa*

Disha Srivastava,^{a*} Jin Seo,^{a*} Binayak Rimal,^b  Sung Joon Kim,^c Stephanie Zhen,^a  Andrew J. Darwin^a

^aDepartment of Microbiology, New York University School of Medicine, New York, New York, USA

^bInstitute of Biomedical Studies, Baylor University, Waco, Texas, USA

^cDepartment of Chemistry and Biochemistry, Baylor University, Waco, Texas, USA

ABSTRACT Carboxy-terminal processing proteases (CTPs) occur in all three domains of life. In bacteria, some of them have been associated with virulence. However, the precise roles of bacterial CTPs are poorly understood, and few direct proteolytic substrates have been identified. One bacterial CTP is the CtpA protease of *Pseudomonas aeruginosa*, which is required for type III secretion system (T3SS) function and for virulence in a mouse model of acute pneumonia. Here, we have investigated the function of CtpA in *P. aeruginosa* and identified some of the proteins it cleaves. We discovered that CtpA forms a complex with a previously uncharacterized protein, which we have named LbcA (lipoprotein binding partner of CtpA). LbcA is required for CtpA activity *in vivo* and promotes its activity *in vitro*. We have also identified four proteolytic substrates of CtpA, all of which are uncharacterized proteins predicted to cleave the peptide cross-links within peptidoglycan. Consistent with this, a *ctpA* null mutant was found to have fewer peptidoglycan cross-links than the wild type and grew slowly in salt-free medium. Intriguingly, the accumulation of just one of the CtpA substrates was required for some Δ *ctpA* mutant phenotypes, including the defective T3SS. We propose that LbcA-CtpA is a proteolytic complex in the *P. aeruginosa* cell envelope, which controls the activity of several peptidoglycan cross-link hydrolases by degrading them. Furthermore, based on these and other findings, we suggest that many bacterial CTPs might be similarly controlled by partner proteins as part of a widespread mechanism to control peptidoglycan hydrolase activity.

IMPORTANCE Bacterial carboxy-terminal processing proteases (CTPs) are widely conserved and have been associated with the virulence of several species. However, their roles are poorly understood, and few direct substrates have been identified in any species. *Pseudomonas aeruginosa* is an important human pathogen in which one CTP, known as CtpA, is required for type III secretion system function and for virulence. This work provides an important advance by showing that CtpA works with a previously uncharacterized binding partner to degrade four substrates. These substrates are all predicted to hydrolyze peptidoglycan cross-links, suggesting that the CtpA complex is an important control mechanism for peptidoglycan hydrolysis. This is likely to emerge as a widespread mechanism used by diverse bacteria to control some of their peptidoglycan hydrolases. This is significant, given the links between CTPs and virulence in several pathogens and the importance of peptidoglycan remodeling to almost all bacterial cells.

KEYWORDS *Pseudomonas aeruginosa*, cell envelope, cell wall, peptidoglycan hydrolases, proteases

Pseudomonas aeruginosa is a Gram-negative bacterium that accounts for over 10% of health care-associated infections with an identifiable cause (1). In acute infections, *P. aeruginosa* utilizes a type III secretion system (T3SS) to export proteins into host

Received 1 May 2018 Accepted 8 May 2018 Published 17 July 2018

Citation Srivastava D, Seo J, Rimal B, Kim SJ, Zhen S, Darwin AJ. 2018. A proteolytic complex targets multiple cell wall hydrolases in *Pseudomonas aeruginosa*. mBio 9:e00972-18. <https://doi.org/10.1128/mBio.00972-18>.

Invited Editor Thomas Bernhardt, Harvard Medical School

Editor Howard A. Shuman, University of Chicago

Copyright © 2018 Srivastava et al. This is an open-access article distributed under the terms of the [Creative Commons Attribution 4.0 International license](https://creativecommons.org/licenses/by/4.0/).

Address correspondence to Andrew J. Darwin, andrew.darwin@med.nyu.edu.

* Present address: Disha Srivastava, FCBCURE, Parsippany, New Jersey, USA; Jin Seo, Johnson & Johnson, Inc., Skillman, New Jersey, USA.

cells, where they interfere with signaling and immune function and cause cytotoxicity (2). In chronic infections, *P. aeruginosa* forms biofilms resilient to clearance by antibiotics and the immune response (3, 4). The emergence of antibiotic-resistant strains is increasing, making this pathogen a top priority for the discovery of new therapeutic targets (5).

Proteases are important virulence factors for many pathogens, including *P. aeruginosa* (6). One intriguing family is the carboxy-terminal processing proteases (CTPs), found in all three domains of life. CTPs belong to the S41 family of serine proteases with a serine/lysine catalytic dyad (7). They are believed to target substrates close to their C terminus (8, 9). A well-described CTP occurs in plant chloroplasts and cyanobacteria, where it cleaves a component of the photosystem II reaction center to activate it (10, 11). Gram-negative bacterial CTPs are found exclusively in the periplasmic compartment and have been implicated in cleaving proteins associated with cell envelope function (8, 12). Some CTPs have been associated with virulence, but mostly by poorly defined mechanisms (13–19). Indeed, despite their widespread conservation, our knowledge of how CTPs function and what they cleave is limited.

Escherichia coli has one CTP, known as Prc or Tsp (8, 9). *prc* null mutants have altered cell morphology, increased drug and low osmotic sensitivity, and altered virulence (20, 21). Prc was proposed to process penicillin-binding protein 3 (PBP3 [FtsI]), an essential peptidoglycan transpeptidase required for cell division (8). More recently, another Prc substrate was discovered, the peptidoglycan hydrolase MepS, which cleaves peptide cross-links between the glycan chains of peptidoglycan (22, 23). These substrates suggest that Prc plays a role in controlling different aspects of peptidoglycan metabolism. However, Prc has also been shown to cleave incorrectly folded polypeptides in the periplasm, suggesting that it has a broader role in protein quality control (9, 24, 25). *P. aeruginosa* has a homologue of *E. coli* Prc, with the two proteins sharing over 40% amino acid identity and belonging to the CTP-1 subfamily (7). *P. aeruginosa* Prc has been proposed to contribute to degradation of the anti-sigma factor MucA, which induces the AlgT/U regulon and subsequent production of the exopolysaccharide alginate (26–28).

Unlike *E. coli*, *P. aeruginosa* has a second CTP, CtpA, which is smaller than Prc and in a different subfamily (the CTP-3 subfamily [18, 29]). CtpA is required for T3SS function, and a *ctpA* null mutant is less cytotoxic to cultured cells and attenuated in a mouse model of acute pneumonia (18). We also reported that a Δ *ctpA* mutant is sensitive to mislocalized pore-forming secretin proteins, has increased resistance to two cationic surfactants, and has an altered cell envelope when viewed by electron microscopy, and that CtpA overproduction induces an extracytoplasmic function sigma factor regulon (18). Furthermore, others found that a *ctpA* transposon insertion mutant has reduced swarming motility (30). All of this suggests that CtpA has a significant impact on the cell envelope. Here, we report that CtpA forms a complex with a protein we have named LbcA (lipoprotein binding partner of CtpA). LbcA is required for CtpA activity *in vivo* and promotes its activity *in vitro*. We have also identified four substrates of CtpA, all of which are uncharacterized proteins predicted to cleave the peptide cross-links within peptidoglycan. The accumulation of one of these substrates appears to be needed for some of the most significant phenotypes of a Δ *ctpA* mutant, including the defective T3SS. We argue that many bacterial CTPs might be controlled by partner proteins as part of a widespread mechanism to control peptidoglycan hydrolase activity.

RESULTS

Identification of a CtpA binding partner. We modified the chromosomal *ctpA* gene to encode CtpA-FLAG-His₆, in strains encoding wild-type CtpA or CtpA with catalytic serine 302 mutated to alanine (CtpA-S302A). The rationale was that CtpA-S302A might trap substrates after tandem affinity purification. These experiments were done with or without *in vivo* formaldehyde cross-linking prior to protein purification, but the results were similar, and only an experiment without cross-linking is shown (Fig. 1A).

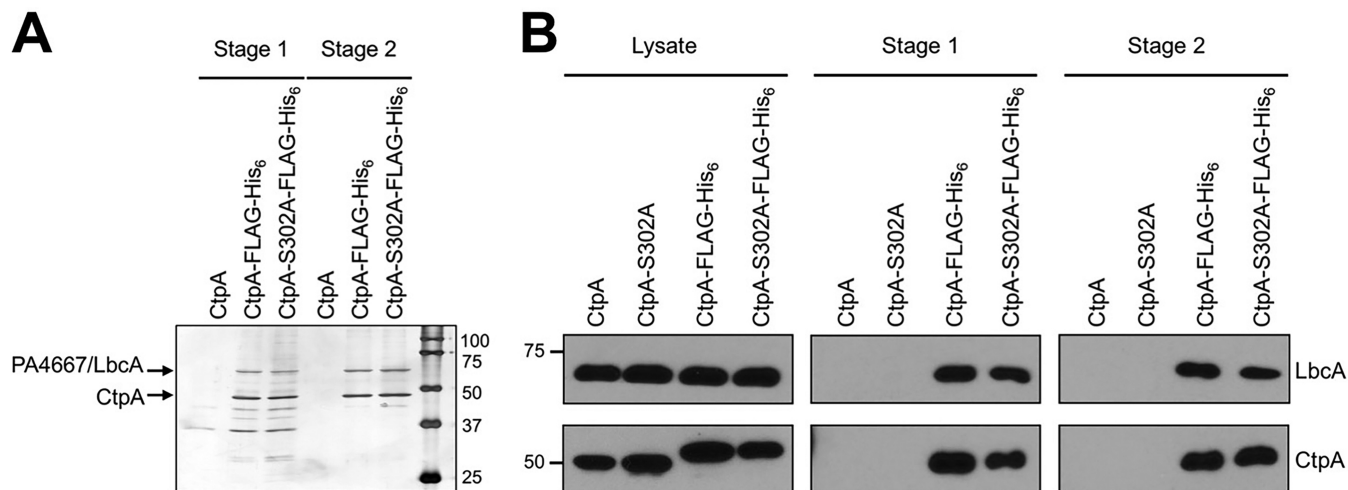


FIG 1 Identification of the CtpA interaction partner PA4667/LbcA. (A) Tandem affinity tag purification. Proteins were purified from detergent-solubilized lysates of the wild-type strain (CtpA) or derivatives encoding CtpA-FLAG-His₆ or the proteolytically inactive CtpA-S302A-FLAG-His₆. Purification was done with nickel agarose (stage 1) followed by anti-FLAG M2 agarose resin (stage 2). Samples were separated on a 12.5% SDS-polyacrylamide gel, which was stained with silver. Molecular mass marker proteins (in kilodaltons) are labeled on the right-hand side. (B) Immunoblot analysis of detergent-solubilized lysate and stage 1 and 2 purified samples, prepared as in panel A. LbcA and CtpA were detected with polyclonal antisera. Strains in which CtpA or CtpA-S302A were not tagged with FLAG-His₆ served as negative controls. Approximate positions of molecular mass marker proteins (in kilodaltons) are indicated on the left-hand side.

Both versions of CtpA copurified with abundant amounts of a protein running between the 50- and 75-kDa markers in SDS-PAGE (Fig. 1A). Mass spectrometry identified it as PA4667 (PAO1 strain designation). A polyclonal antiserum raised against PA4667 confirmed its copurification with epitope-tagged CtpA or CtpA-S302A (Fig. 1B). PA4667 is a predicted 63-kDa outer membrane lipoprotein with 11 tetratricopeptide repeats (TPRs). The TPR motif is a degenerate 34-amino-acid sequence that mediates protein-protein interactions (31). PA4667 does not appear to be a CtpA substrate because its level is similar in *ctpA*⁺ wild-type and Δ *ctpA* mutant strains (see below). Therefore, we will refer to PA4667 as LbcA (lipoprotein binding partner of CtpA).

Δ *lbcA* and Δ *ctpA* mutants have common phenotypes. We hypothesized that LbcA might be required for CtpA function, but we could not construct Δ *lbcA* in-frame deletion mutants. We could make mutants in which *lbcA* was replaced by *aacC1*, encoding gentamicin resistance, but only if *aacC1* was in the same orientation as *lbcA*. *lbcA* is in an operon with the downstream essential genes *lolB* and *ipk* (32). We speculate that the *aacC1* promoter helps to express *lolB-ipk*, and the inability to make a Δ *lbcA* in-frame deletion might be due to reduced *lolB-ipk* expression.

A Δ *ctpA* mutant has a defective T3SS (18). Therefore, we compared the ability of *ctpA* and *lbcA* null mutants to export T3SS effector proteins ExoS and ExoT and found that both were defective (Fig. 2A). The Δ *lbcA::aacC1* mutant was complemented by an *lbcA*⁺ plasmid, and the Δ *ctpA* mutant was complemented by wild-type CtpA, but not by CtpA-S302A (Fig. 2A).

Recently, we discovered that a Δ *ctpA* mutant has a specific phenotype in a commonly used surface attachment assay (33). After an 8-h incubation, the Δ *ctpA* mutant attached robustly, whereas the wild type did not (Fig. 2B). We tested if the *lbcA* null mutant shares this phenotype, and it did (Fig. 2B). After longer incubation, the wild type caught up so that attachment of wild-type and mutant strains was indistinguishable (data not shown). This accelerated attachment phenotype was not caused by faster growth of the mutants in these assays (data not shown).

Evidence that LbcA recruits CtpA to the outer membrane. LbcA is a predicted outer membrane lipoprotein, so it should tether CtpA to the membrane. However, we and others concluded that CtpA is a soluble periplasmic protein because it was released by osmotic shock (18, 29). Even so, some CtpA was not released in our experiment (18). Indeed, we have found that a significant amount of CtpA is always retained, and this is

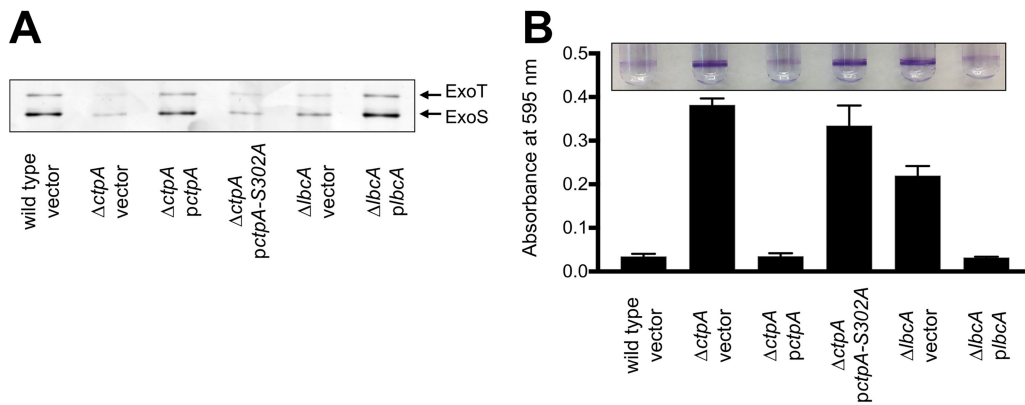


FIG 2 Δ ctpA and Δ lbcA mutants share common phenotypes. (A) T3SS function. Wild-type or Δ ctpA or Δ lbcA mutant strains contained the tac promoter expression plasmid pVLT35 (vector) or derivatives encoding CtpA, CtpA-S302A, or LbcA as indicated. TSB growth medium contained 5 mM EGTA to induce T3SS activity and 10 μ M IPTG to induce the tac promoter of the complementing plasmids. Cell-free supernatants derived from equivalent amounts of cells were separated on an SDS-PAGE gel, which was stained with silver. The region with the abundant T3SS effectors ExoT and ExoS is shown. (B) Surface attachment. The same strains as in panel A were incubated in glass test tubes at 30°C without agitation for 8 h. The growth medium contained 10 μ M IPTG to induce the tac promoter of the complementing plasmids. Bacterial cells attached to the glass at the air-liquid interface were stained with crystal violet (purple rings). The stain was dissolved in ethanol and quantified by measuring absorbance at 595 nm. All strains were tested in triplicate, and error bars represent the standard deviation from the mean.

more pronounced when cultures are harvested at a lower optical density (OD) than before (OD at 600 nm [OD₆₀₀] of 1 instead of 1.5). Therefore, we osmotically shocked *lbcA*⁺ and Δ lbcA strains grown to an OD₆₀₀ of 1. In the *lbcA*⁺ strain, most CtpA was retained, whereas a soluble periplasmic control protein was released (Fig. 3A). However, in a Δ lbcA mutant, CtpA was released. This supports the hypothesis that LbcA influences CtpA localization.

We also separated cells into soluble and insoluble fractions by lysis and ultracentrifugation. Interestingly, LbcA was found in the soluble and insoluble fractions (Fig. 3B). We do not know if this is physiologically significant or an artifact resulting from LbcA being solubilized during sample processing. Regardless, in an *lbcA*⁺ strain, CtpA fractionated identically to LbcA, whereas in a Δ lbcA mutant, CtpA was only in the

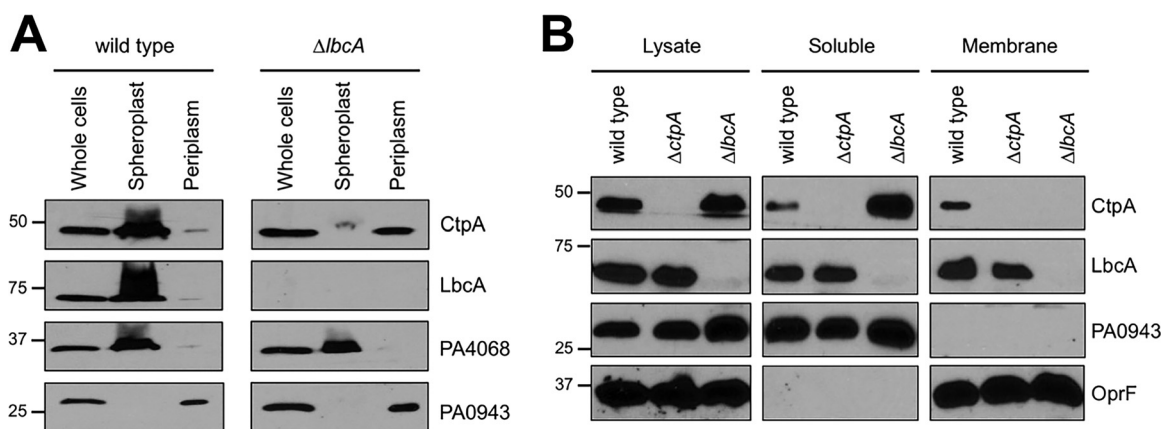


FIG 3 LbcA promotes retention of CtpA in spheroplast and membrane fractions. (A) Osmotic shock fractionation. Total cell lysate (whole cells), as well as spheroplast and periplasm fractions generated by osmotic shock, was separated by SDS-PAGE and transferred to nitrocellulose, and proteins were detected with polyclonal antisera. PA0943 is a soluble periplasmic protein control, and PA4068 is a cytoplasmic spheroplast retention control (51). (B) Fractionation of lysed cells. Cells were lysed by two passages through a French pressure cell and separated into soluble and insoluble (membrane) fractions by ultracentrifugation. Samples derived from equivalent amounts of cells were separated by SDS-PAGE and transferred to nitrocellulose, and proteins were detected with polyclonal antisera. PA0943 is a soluble protein control, and OprF is an insoluble outer membrane control.

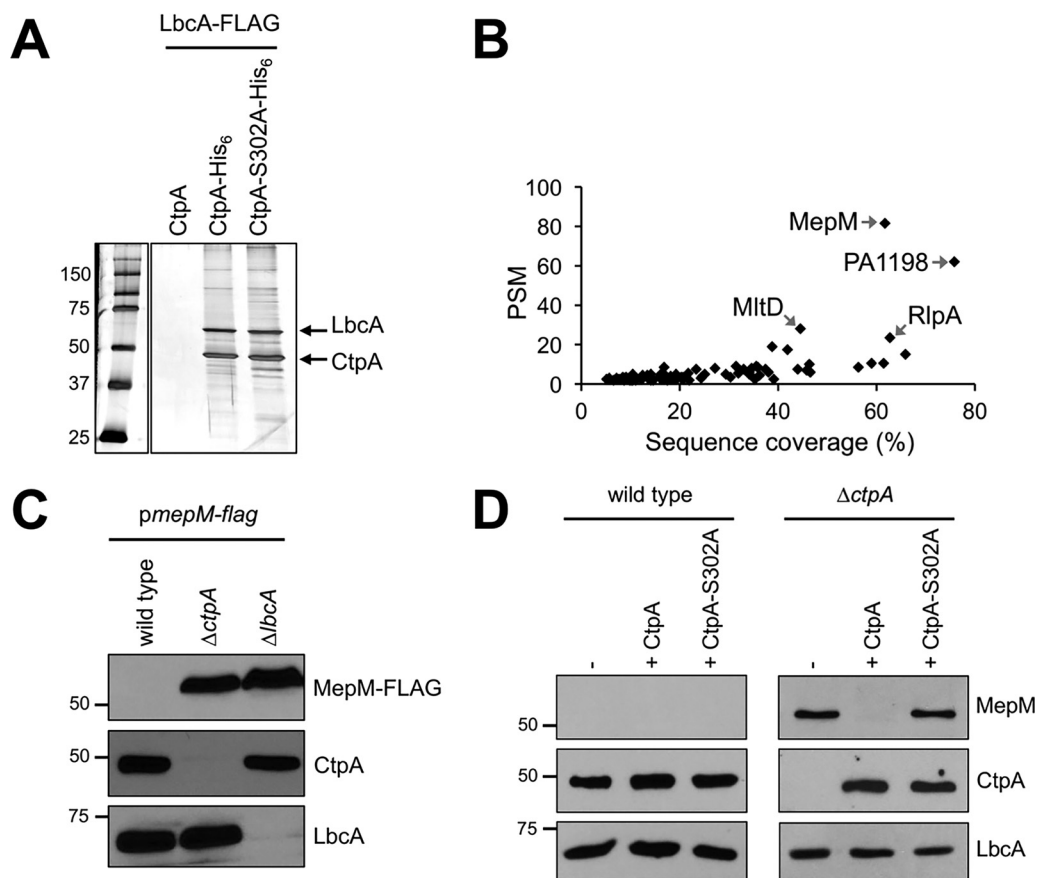


FIG 4 Identification of MepM as a putative substrate of the LbcA-CtpA proteolytic complex. (A) Tandem affinity tag purification. Proteins were purified from detergent-solubilized lysates of $\Delta ctpA$ strains. All strains had a plasmid encoding LbcA-FLAG, as well as a second plasmid encoding untagged CtpA (negative control), CtpA-His₆, or the proteolytically inactive CtpA-S302A-His₆. Purification was done with nickel agarose followed by anti-FLAG M2 agarose resin. Samples were separated on a 12.5% SDS-polyacrylamide gel, which was stained with silver. Molecular mass marker proteins (in kilodaltons) are labeled on the left-hand side. An irrelevant region of the gel between the marker and sample lanes has been removed. (B) Scatterplot of proteins identified by mass spectrometry after purification from strains encoding CtpA-S302A-His₆. Data are the average peptide spectrum matches (PSMs) and sequence coverage from duplicate purifications from strains with CtpA-S302A-His₆. Each point represents a different protein. All proteins plotted were detected in both of the LbcA-CtpA-S302A purifications but neither of duplicate LbcA-CtpA purifications. (C) Immunoblot analysis of equivalent amounts of whole-cell lysates of the wild-type or $\Delta ctpA$ and $\Delta lbcA$ mutant strains. All strains contained an arabinose-inducible expression plasmid encoding MepM-FLAG and were grown in medium containing 0.2% (wt/vol) arabinose. Approximate positions of molecular mass marker proteins (in kilodaltons) are indicated on the left-hand side. MepM-FLAG was detected with anti-FLAG monoclonal antibodies, and CtpA and LbcA were detected with polyclonal antisera. (D) Detection of endogenous MepM. Shown are results from immunoblot analysis of equivalent amounts of whole-cell lysates of the wild-type and $\Delta ctpA$ strains. Strains contained the *tac* promoter expression plasmid pVLT35 (–) or derivatives encoding CtpA or CtpA-S302A, as indicated. Approximate positions of molecular mass marker proteins (in kilodaltons) are indicated on the left-hand side. MepM, CtpA, and LbcA were detected with polyclonal antisera.

soluble fraction (Fig. 3B). This is consistent with an LbcA-CtpA interaction tethering some CtpA to the outer membrane.

Isolation of a putative CtpA substrate. To find substrates of the LbcA-CtpA complex, we modified our tandem affinity tag approach by putting the His₆ tag on CtpA or CtpA-S302A and the FLAG tag on LbcA. Strains were grown under T3SS-inducing conditions and treated with formaldehyde to cross-link associated proteins. Proteins were purified using nickel agarose followed by anti-FLAG affinity gel and analyzed by SDS-PAGE (Fig. 4A). We also analyzed two independent purifications from each strain by mass spectrometry. A total of 101 proteins were present in both LbcA-CtpA-S302A samples, but neither LbcA-CtpA sample (Fig. 4B; see Table S1 in the supplemental material). We focused on the most abundant protein according to peptide spectrum matches (PSMs), the uncharacterized PA0667 (Fig. 4B). PA0667 has a

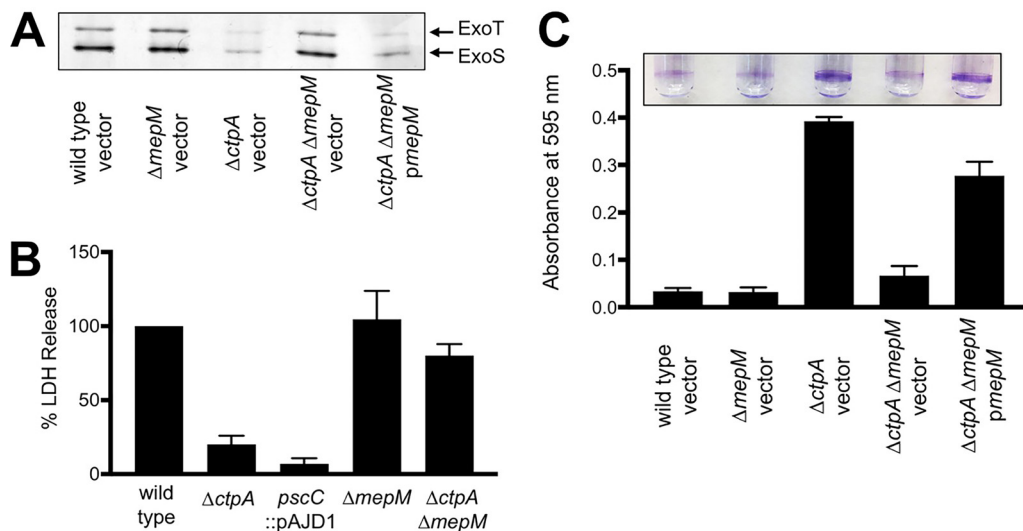


FIG 5 An *mepM* null mutation suppresses $\Delta ctpA$ phenotypes. (A) T3SS function. Wild-type or $\Delta mepM$, $\Delta ctpA$ or $\Delta ctpA \Delta mepM$ mutant strains contained the *araBp* promoter expression plasmid pHERD20T (vector) or a derivative encoding MepM as indicated. TSB growth medium contained 1 mM EGTA to induce T3SS activity and 0.02% arabinose to induce the *araB* promoter of pHERD20T. Cell-free supernatants derived from equivalent amounts of cells were separated with SDS-PAGE gel, which was stained with silver. The region with the abundant T3SS effectors ExoT and ExoS is shown. (B) Cytotoxicity to CHO-K1 cells. Strains with the indicated genotypes were added to CHO-K1 cells at a multiplicity of infection of ~10 and incubated for 4 h. Cell-free supernatants were then analyzed for lactate dehydrogenase (LDH) content. The amount of LDH in the supernatant following incubation with the wild-type strain was set to 100%, and the values for the mutants are shown as the relative percentage. Data were averaged from three independent experiments, with error bars showing the standard deviation from the mean. (C) Surface attachment. The same strains from panel A were incubated in glass test tubes at 30°C without agitation for 8 h. The growth medium contained 0.02% arabinose to induce the *araB* promoter of the complementing plasmids. Bacterial cells attached to the glass at the air-liquid interface were stained with crystal violet (purple rings). The stain was dissolved in ethanol and quantified by measuring absorbance at 595 nm. All strains were tested in triplicate, and error bars represent the standard deviation from the mean.

Sec-dependent signal sequence, an LysM peptidoglycan-binding domain, and an LysM/M23 peptidase domain. It is 35% identical to *E. coli* MepM, a DD-endopeptidase that cleaves D-Ala-meso-diaminopimelic acid (DAP) peptide peptidoglycan cross-links (23). Therefore, we will refer to PA0667 as MepM.

Evidence that MepM is a substrate of the LbcA-CtpA complex *in vivo*. To test if MepM might be an LbcA-CtpA substrate, we constructed a plasmid encoding arabinose-inducible MepM-FLAG. After growth in the presence of arabinose, the MepM-FLAG protein was undetectable in the wild-type strain, whereas it was abundant in $\Delta ctpA$ and $\Delta lbcA$ mutants (Fig. 4C). To analyze endogenous MepM, we raised a polyclonal antiserum against it. This antiserum did not detect MepM in the wild-type strain, but once again it revealed MepM accumulated in a $\Delta ctpA$ mutant (Fig. 4D). This accumulation was reversed by a plasmid encoding wild-type CtpA, but not by CtpA-S302A (Fig. 4D). These data suggest that MepM is cleaved by CtpA *in vivo*.

Deletion of *mepM* suppresses $\Delta ctpA$ mutant phenotypes. $\Delta ctpA$ phenotypes might be caused by MepM accumulation. If so, a $\Delta mepM$ mutation should suppress them. To test this, we introduced an *mepM* in-frame deletion mutation into the wild-type and $\Delta ctpA$ strains and surveyed their phenotypes (Fig. 5).

First, we monitored T3SS function. The $\Delta mepM$ mutation alone did not affect ExoS/T export (Fig. 5A), whereas a $\Delta ctpA$ mutant exported smaller amounts, as reported before (18). However, the $\Delta ctpA$ phenotype was suppressed by a $\Delta mepM$ mutation, with the ExoS/T secretion profiles of wild-type and $\Delta ctpA \Delta mepM$ strains being indistinguishable (Fig. 5A). Furthermore, *mepM* expression from a plasmid reduced T3SS function in the $\Delta ctpA \Delta mepM$ mutant (Fig. 5A). These data suggest that MepM accumulation was responsible for the defective T3SS of the $\Delta ctpA$ mutant.

We also investigated cytotoxicity toward CHO-K1 cells by measuring lactate dehydrogenase (LDH) release. This is an established model for studying the toxic effect of

the *P. aeruginosa* T3SS on eukaryotic cells (18, 34). The cytotoxicity phenotypes of the $\Delta ctpA$, $\Delta mepM$, and $\Delta ctpA \Delta mepM$ strains were consistent with their T3SS phenotypes (Fig. 5A and B). $\Delta mepM$ did not affect cytotoxicity, but $\Delta ctpA$ reduced it, and this reduction was suppressed in the $\Delta ctpA \Delta mepM$ double mutant (Fig. 5B).

Finally, the $\Delta mepM$ mutation also suppressed the accelerated surface attachment phenotype of a $\Delta ctpA$ mutant, and this suppression was reversed by an $mepM^+$ plasmid (Fig. 5C). Together, all these findings suggest that many phenotypes of a $\Delta ctpA$ mutant require MepM. As expected, a $\Delta mepM$ mutation also suppressed these phenotypes of a $\Delta lbcA$ mutant (data not shown). Therefore, we hypothesized that the phenotypes of LbcA-CtpA-defective strains are the result of increased hydrolysis of peptidoglycan cross-links, which we tested next.

Peptidoglycan cross-linking is reduced in a $\Delta ctpA$ mutant. The peptidoglycan compositions of the wild-type and $\Delta ctpA$ strains were characterized by mass spectrometry. The repeat unit consists of the disaccharide GlcNAc-MurNAc with a pentapeptide stem, L-Ala-D-iso-Gln-m-DAP-D-Ala-D-Ala, attached to the lactic moiety of MurNAc (Fig. 6A). The disaccharides are joined by β_{1-4} glycosidic linkages to form the glycan chain. The glycan chains are cross-linked via a peptide bond between the side chain of m-DAP in an acceptor stem of one repeat unit, to the carbonyl carbon of a penultimate D-Ala in a donor stem of a neighboring glycan chain. Cell walls were digested with mutanolysin, which cleaves the β_{1-4} glycosidic linkage between MurNAc and GlcNAc, resulting in muropeptide fragments with intact cross-links. Muropeptide ions were identified by matching the observed m/z values to the corresponding entries in a muropeptide library generated *in silico* using an in-house program. Forty-seven unique muropeptide ion species from the wild type and 33 from the $\Delta ctpA$ mutant were selected for the analysis. Muropeptide fragments were quantified by integrating the extracted ion chromatogram (XIC) of the selected muropeptide ion (35–37). The normalized summed integrals of muropeptides from the XIC ion current were categorized based on the cross-link number per muropeptide fragment (Fig. 6B). Muropeptide fragments larger than trimers were not observed, and the most abundant muropeptides were dimers. Representative spectra of the monomer, dimer, and trimer from the wild type are shown in Fig. 6, and the chemical structure and calculated masses are shown in Fig. S1 in the supplemental material.

The cell walls of the $\Delta ctpA$ mutant had a reduced concentration of peptidoglycan dimers ($75.85\% \pm 3.90\%$) compared to the wild type ($87.30\% \pm 1.34\%$) and a concomitant increase in monomers (Fig. 6B). This is consistent with decreased peptidoglycan cross-linking efficiency (ρ_{CL}) in the $\Delta ctpA$ mutant. The calculated ρ_{CL} values for the wild type and $\Delta ctpA$ mutant were 50.86% and 49.46%, respectively (Fig. 6C). The reduced cross-linking efficiency in the $\Delta ctpA$ mutant is small. However, the accompanying increase in trimers and monomers indicates altered peptidoglycan biosynthesis. A small effect was expected because a $ctpA$ mutant grows well, had few phenotypes in a Biolog Phenotype MicroArray (18), and is only slightly sensitive to low-osmosis conditions (described below). Regardless, these data are consistent with the accumulation of peptidoglycan cross-link hydrolase activity in LbcA-CtpA-defective strains.

LbcA enhances CtpA-dependent degradation of MepM *in vitro*. To test if MepM is a direct substrate of CtpA, we purified C-terminal hexahistidine-tagged proteins. MepM was stable when incubated alone, but in the presence of CtpA, the amount of MepM decreased (Fig. 7A). Furthermore, when MepM was incubated with both CtpA and LbcA it became undetectable, which is consistent with LbcA enhancing CtpA-dependent degradation (Fig. 7A). There was no MepM degradation when it was incubated with CtpA-S302A \pm LbcA. This supports the contentions that the S302A mutation destroys CtpA activity, that MepM degradation was due to CtpA and not a contaminating protease activity, and that LbcA cannot degrade MepM itself.

We also monitored the CtpA-dependent degradation of MepM over time and found that it was faster in the presence of LbcA (Fig. 7B). Finally, we incubated CtpA with another LytM/M23 peptidase domain protein, PA3787. However, PA3787 was not

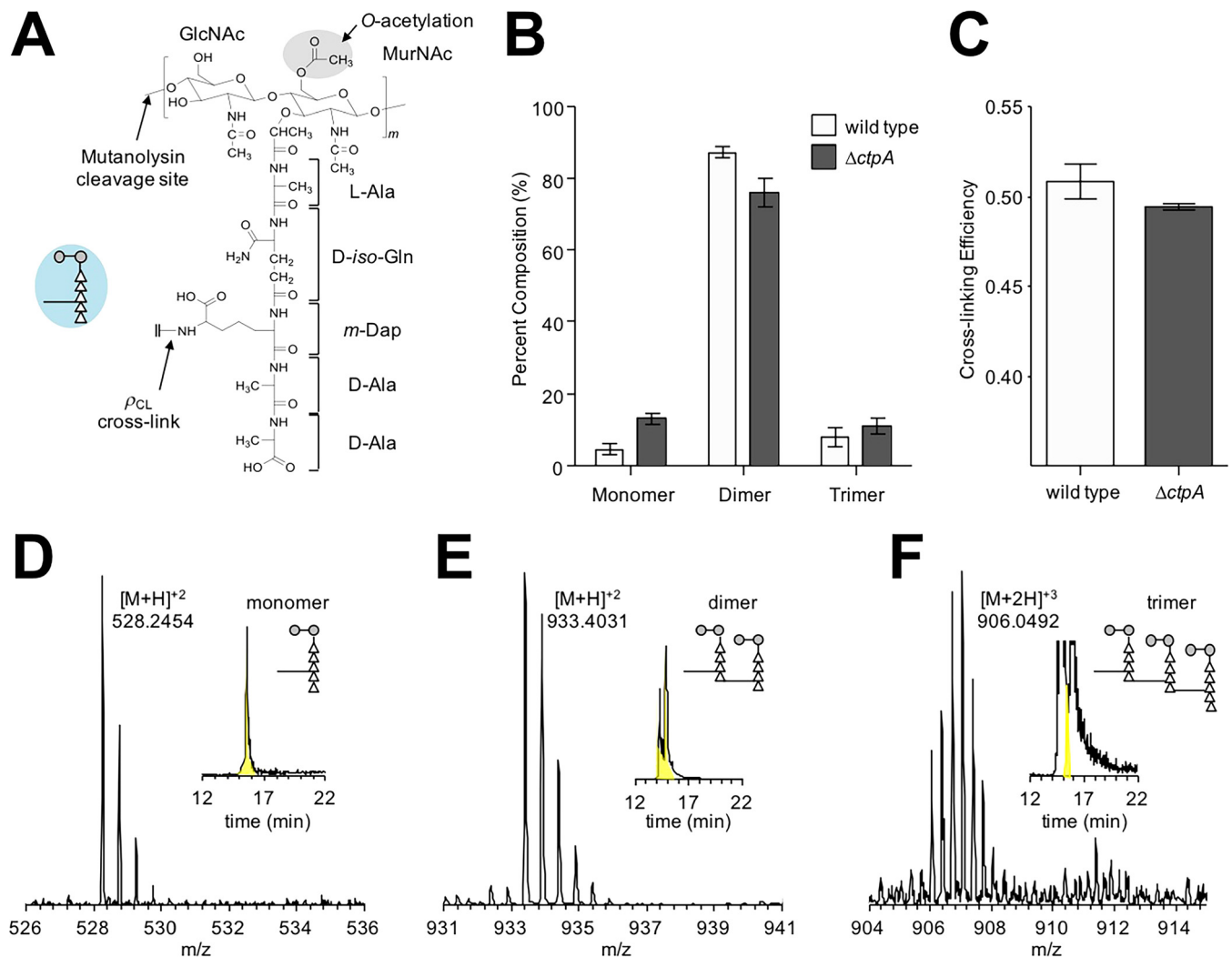


FIG 6 Changes in peptidoglycan composition of a $\Delta ctpA$ mutant. (A) Chemical structure of the peptidoglycan repeat unit in *P. aeruginosa*. The disaccharide of the peptidoglycan repeat unit is shown with two modifications: O-acetylation of MurNAc at the C-6 position and amidation of D-iso-Glu in the peptide stem to D-iso-Gln. The interpeptide bridge structure in *P. aeruginosa* is m-DAP. A schematic representation of a peptidoglycan repeat unit is shown as a figure inset with the disaccharide as gray-filled circles, the amino acids in the pentapeptide stem as open triangles, and the interpeptide bridge structure as a line. The polymerized peptidoglycans are cross-linked by forming a peptide bond between the side chain of m-DAP from one repeat unit to the carbonyl carbon of penultimate D-Ala of a peptidoglycan stem from a neighboring glycan chain. (B) The mutanolysin-digested muropeptide fragments were characterized by LC-MS. Forty-seven unique muropeptide ions from the wild type and 33 from the $\Delta ctpA$ mutant were identified from LC-MS, and each muropeptide was quantified by integrating the extracted ion chromatogram (XIC) of the selected muropeptide ion. Peptidoglycan dimers are the most abundant muropeptides found in both the wild type and $\Delta ctpA$ mutant, with compositions of 87.30% ± 1.34% and 75.85% ± 3.90%, respectively. Muropeptide fragments larger than trimers were not observed. The *P* values for the differences between the wild-type and $\Delta ctpA$ strains for monomers, dimers, and trimers based on the *t* test are 0.0001, 0.0003, and 0.0216, respectively. (C) The calculated peptidoglycan cross-linking efficiencies (ρ_{CL}) for the wild type and $\Delta ctpA$ mutant are 50.86% ± 0.98% and 49.46% ± 0.18%, respectively, with a *P* value of 0.0038. All errors bars represent the 95% confidence interval (*n* = 3). Representative mass spectra of monomer (D), dimer (E), and trimer (F) are shown with the XICs as insets. The corresponding chemical structures are shown in Fig. S1.

degraded significantly, showing that CtpA has substrate specificity (Fig. 7B). These *in vitro* experiments support the characterization of MepM as a direct substrate of CtpA and suggest that LbcA catalyzes the proteolysis.

The LbcA-CtpA complex degrades additional peptidoglycan cross-link hydrolases. MepM was the most abundant protein copurified with LbcA-CtpA-S302A. Remarkably, the three proteins with the next highest PSMs are also known or predicted peptidoglycan hydrolases (PA1198, MltD, and RlpA) (Fig. 4B). PA1198 is homologous to *E. coli* NlpC/P60 peptidase family member MepS, a DD-endopeptidase that targets the same peptidoglycan cross-links as MepM (23). MltD and RlpA are lytic transglycosylases that attack the glycan chain (38–40).

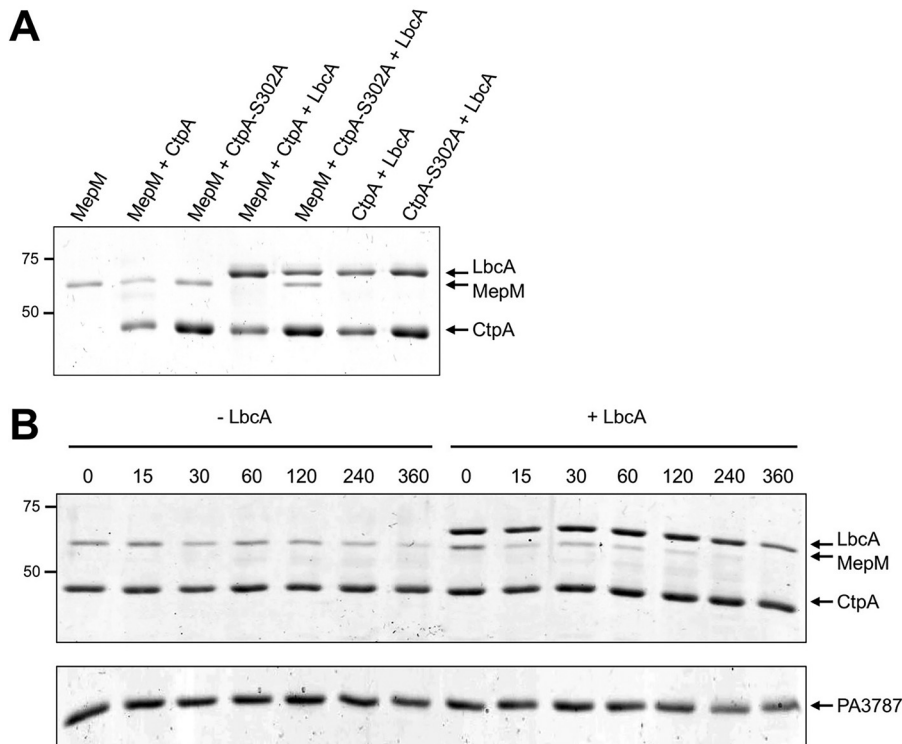


FIG 7 *In vitro* proteolysis of MepM. (A) CtpA degrades MepM and is enhanced by LbcA. 2 μ M concentrations of the indicated C-terminal His₆-tagged proteins was incubated for 3 h at 37°C. Samples were separated on a 12.5% SDS-PAGE gel, which was stained with Coomassie brilliant blue. Approximate positions of molecular mass marker proteins (in kilodaltons) are indicated on the left-hand side. (B) Time course. Reaction mixtures contained 2 μ M CtpA-His₆ and MepM-His₆ either without (-LbcA) or with (+LbcA) 2 μ M LbcA-His₆. Reactions were terminated at the indicated time points (minutes) by adding SDS-PAGE sample buffer and boiling. As a negative control, the same experiment was done using PA3787 in place of MepM. Samples were separated on 12.5% SDS-PAGE gels, which were stained with Coomassie brilliant blue. Approximate positions of molecular mass marker proteins (in kilodaltons) are indicated on the left-hand side. PA3787 ran at the midway point between marker proteins of 37 and 25 kDa, which were above and below, respectively, the region of the gel shown in the figure.

To test if CtpA might cleave these putative peptidoglycan hydrolases, we constructed plasmids encoding arabinose-inducible FLAG-tagged versions. PA1198-FLAG was undetectable in the wild type, whereas it became abundant in a Δ *ctpA* mutant (Fig. 8A). We extended the PA1198 analysis to a Δ *lbcA* mutant, in which it also accumulated (Fig. 8A). Therefore, PA1198 might also be an LbcA-CtpA substrate. However, MltD-FLAG and RlpA-FLAG were detectable in wild-type strains and did not accumulate in a Δ *ctpA* mutant (Fig. 8A). This suggests that MltD and RlpA are not CtpA substrates (see Discussion).

We also used a biased approach by screening some putative *P. aeruginosa* peptidoglycan hydrolases. Again, this was done by constructing plasmids encoding arabinose-inducible FLAG-tagged versions. Candidates included three members of the LytM/M23 peptidase family that MepM is in (PA3787, PA4404, and PA5551), two members of the LytM/M23 family with predicted defective peptidase domains (PA3623/NlpD and PA5363), and three members of the NlpC/P60 family that PA1198 is in (PA0639, PA1199, and PA1844/Tse1). We also tested PA2272 (PBP3A) and PA4418 (PBP3), two homologues of *E. coli* penicillin-binding protein 3 (PBP3/FtsI), which has been proposed to be proteolytically processed by its CTP, Prc/Tsp (8). Most of these candidates did not accumulate in a Δ *ctpA* mutant, suggesting that they are not substrates (Fig. 8A). However, PA1199 and PA4404 were not detected in the wild type but accumulated in the Δ *ctpA* mutant. We extended their analysis to a Δ *lbcA* mutant, in which they also accumulated (Fig. 8A). Therefore, PA1199 and PA4404 are also putative LbcA-CtpA proteolytic substrates.

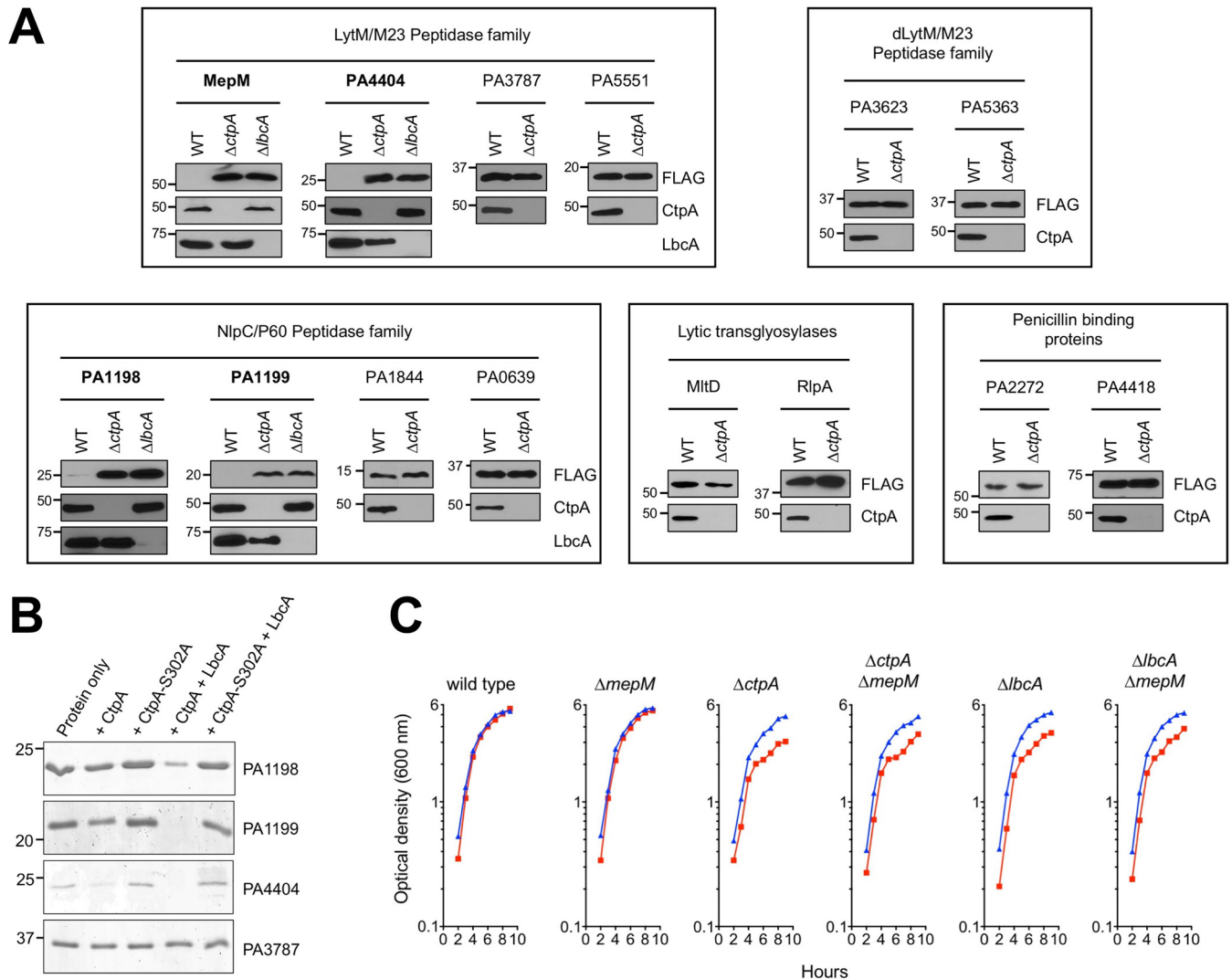


FIG 8 Evidence that the LbcA-CtpA complex has additional substrates. (A) *In vivo* analysis. Shown are results from immunoblot analysis of equivalent amounts of whole-cell lysates of the wild-type and $\Delta ctpA$ strains and also of $\Delta lbcA$ strains that accumulated in the $\Delta ctpA$ mutant. All strains contained an arabinose-inducible expression plasmid encoding C-terminal FLAG-tagged versions of the indicated proteins. Approximate positions of molecular mass marker proteins (in kilodaltons) are indicated on the left-hand side. Test proteins were detected with anti-FLAG monoclonal antibodies, and CtpA and LbcA were detected with polyclonal antisera. Each box has analysis of proteins in related families, as indicated at the top. Only those proteins with names in boldface accumulated in the $\Delta ctpA$ mutant. (B) *In vitro* analysis. $2 \mu\text{M}$ concentrations of the indicated C-terminal His₆-tagged proteins were incubated for 3 h at 37°C. "Protein only" indicates incubation of the test substrate alone. PA3787-His₆ was used as a negative control. Samples were separated on a 15% SDS-PAGE gel, which was stained with Coomassie brilliant blue. Approximate positions of molecular mass marker proteins (in kilodaltons) are indicated on the left-hand side. (C) Sensitivity of $\Delta ctpA$ and $\Delta lbcA$ mutants to low-salt conditions is not suppressed by $\Delta mepM$. Strains were grown at 37°C in LB broth containing 1% (wt/vol) NaCl (blue) or no NaCl (red). Optical density was measured hourly.

To confirm PA1198, PA1199, and PA4404 as CtpA substrates, we purified hexahistidine-tagged versions and tested them *in vitro*. All were degraded when incubated with LbcA and CtpA, but there was no degradation by CtpA-S302A (Fig. 8B). Therefore, CtpA degrades two peptidoglycan hydrolases in the LytM/M23 peptidase family (MepM and PA4404) and two in the NlpC/P60 family (PA1198 and PA1199). Their sequences predict all to be in the cell envelope—MepM as a peptidoglycan-associated protein and PA1198, PA1199, and PA4404 as outer membrane lipoproteins. Furthermore, all are predicted to cleave the peptide cross-links of peptidoglycan. Breaking these cross-links poses a danger to the bacterial cell, and the LbcA-CtpA complex might be an important control mechanism used by *P. aeruginosa* to regulate this activity.

LbcA-CtpA-defective strains grow poorly in salt-free medium. *E. coli prc* mutants have altered cell morphology and increased sensitivity to some drugs and low osmo-

larity (20). Biolog Phenotype MicroArray analysis of a *P. aeruginosa* $\Delta ctpA$ mutant revealed no increased drug sensitivity (18). We have examined cells by light microscopy after growth at 37°C or 42°C in media with or without salt and in the exponential and stationary phases, but $\Delta ctpA$ and $\Delta lbcA$ mutations did not noticeably affect cell shape or length (data not shown). This is not surprising because Prc and CtpA have different substrates. (Prc processes FtsI, which might contribute to filamentation of Δprc cells, whereas CtpA does not appear to process *P. aeruginosa* FtsI homologues [Fig. 8A].) Also, *P. aeruginosa* has another CTP (PA3257/AlgO) that is a closer homologue of *E. coli* Prc than is CtpA. Even so, if multiple peptidoglycan hydrolases accumulate in $\Delta ctpA$ or $\Delta lbcA$ mutants (Fig. 8A) and peptidoglycan cross-linking is compromised (Fig. 6), then sensitivity to low osmolarity is expected. Therefore, we also investigated this possibility.

$\Delta ctpA$ and $\Delta lbcA$ mutants grew more slowly than the wild type in Luria-Bertani (LB) broth without NaCl (Fig. 8C). This phenotype was not exacerbated at 42°C and/or on agar (data not shown). Regardless, the occurrence and subtle nature of this phenotype are consistent with the slightly reduced peptidoglycan cross-linking efficiency (Fig. 6). Importantly, this phenotype was not fully suppressed by a $\Delta mepM$ mutation, which further supports the LbcA-CtpA complex degrading multiple peptidoglycan hydrolases.

DISCUSSION

We have discovered that *P. aeruginosa* CtpA forms a complex with LbcA, and both proteins are required for CtpA-mediated proteolysis *in vivo* and *in vitro*. We identified four proteolytic substrates, all of which are predicted to cleave the cross-links between peptidoglycan chains. Therefore, the LbcA-CtpA complex might be an important control mechanism used by *P. aeruginosa* to regulate peptidoglycan cross-link hydrolysis. It has been difficult to investigate if substrate degradation is regulated, because substrates are difficult to detect in protease-competent strains (e.g., Fig. 4 and 8). However, even though CtpA and LbcA protein levels appear constant regardless of growth stage, our preliminary evidence suggests that at least one substrate might be degraded at different rates (D. Srivastava and A. J. Darwin, unpublished data). How this occurs and the signal(s) involved are intriguing future questions.

An exciting parallel exists between the complex we have discovered and the Nlpl-Prc complex in *E. coli*. Prc is a CTP, and Nlpl is an outer membrane lipoprotein with TPR motifs, and together they degrade one peptidoglycan hydrolase, MepS (22). The similarities to LbcA-CtpA are obvious. However, Prc and CtpA are evolutionarily divergent, differing in size by approximately 30 kDa and belonging to different CTP subfamilies. Although Nlpl and LbcA are both outer membrane lipoproteins containing short TPR motifs, their primary sequences are not similar, and LbcA is much larger than Nlpl. In the *E. coli* Nlpl-Prc complex, an Nlpl homodimer binds two Prc monomers to create docking sites for the MepS substrate (41). The LbcA-CtpA complex in *P. aeruginosa* could have similarities to this, but we suspect that its stoichiometry and functioning will have differences due to the divergence of the proteins involved. Regardless, it is important that two very different CTPs and two very different lipoproteins form complexes in two divergent bacterial species to degrade peptidoglycan hydrolases. This suggests that this could be a widespread phenomenon, and a new paradigm might emerge in which many bacterial CTPs work with partner proteins to target cell wall hydrolases.

LbcA-CtpA degrades four predicted peptidoglycan cross-link hydrolases (Fig. 4 and Fig. 7 to 9). Consistent with this, a $\Delta ctpA$ mutant has a cell envelope structural defect when viewed by electron microscopy (18), peptidoglycan cross-linking is reduced (Fig. 6), and it grows poorly in LB broth without NaCl (Fig. 8C). All of this suggests a weakened cell wall caused by increased peptidoglycan cross-link hydrolase activity. Removing the MepM substrate did not suppress the slow growth of $\Delta ctpA$ and $\Delta lbcA$ mutants in salt-free medium (Fig. 8C). This indicates that at least one other CtpA substrate must contribute to this phenotype. In fact, although it is not obvious from the growth curves, the $\Delta mepM$ mutation did improve growth very slightly. Therefore, we hypothesize that the poor growth in LB broth without NaCl results from the combined

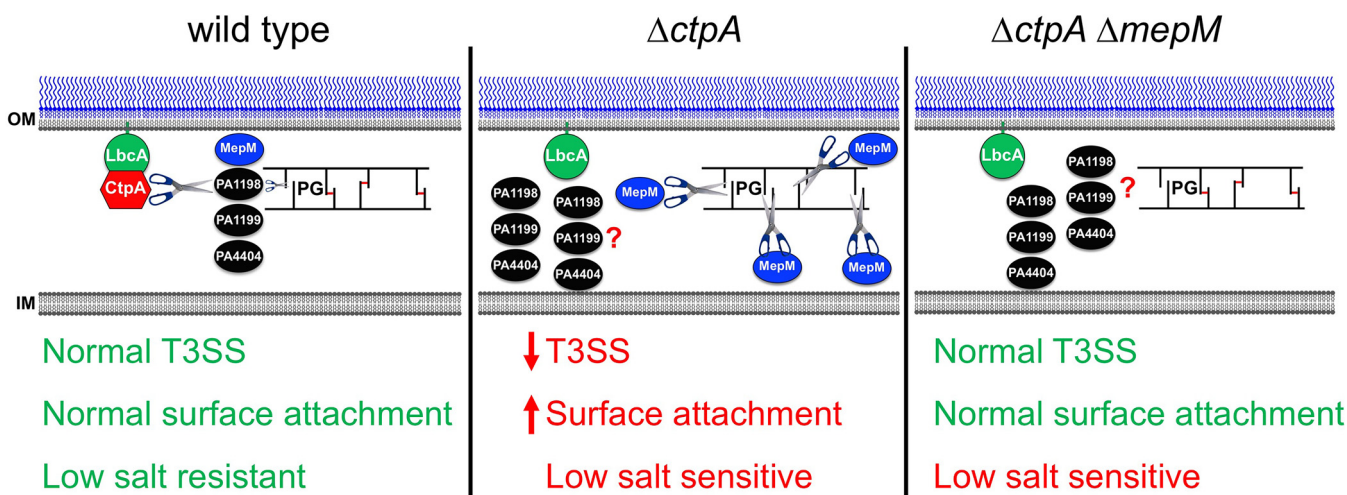


FIG 9 Summary. In a wild-type strain, CtpA forms a complex with the outer membrane lipoprotein LbcA, which is required for CtpA to cleave its targets. The LbcA-CtpA complex can degrade at least four enzymes predicted to cleave peptidoglycan cross-links (MepM, PA1198, PA1199, and PA4404). This might provide a mechanism to carefully constrain cross-link hydrolysis, limiting it to the amount needed for roles such as cell elongation and/or division. In a $\Delta ctpA$ mutant, the peptidoglycan hydrolases can accumulate, which causes excessive cross-link cleavage and subsequent phenotypes, including a defective T3SS, enhanced surface attachment, and low-salt sensitivity. When *mepM* is deleted from the $\Delta ctpA$ mutant, the T3SS and surface attachment phenotypes revert back to wild type, suggesting that elevated MepM activity was their primary cause. However, low-salt sensitivity of a $\Delta ctpA$ mutant is not suppressed by $\Delta mepM$, suggesting that increased activity of one or more of the other substrates is also compromising cell wall integrity. OM, outer membrane; IM, inner membrane.

effect on the cell wall of two or more accumulating CtpA substrates. We have not yet been able to make null mutants of the other CtpA substrates, but a future goal is to investigate their roles.

The defective T3SS and accelerated surface attachment phenotypes of a $\Delta ctpA$ mutant are most likely to be secondary consequences of a compromised cell wall. However, these phenotypes were efficiently suppressed by a $\Delta mepM$ mutation. MepM was the most abundant protein trapped by the LbcA-CtpA-S302A complex (Fig. 4B), and so it might be having the largest influence on the cell wall. If so, even though removal of MepM might not fix all the cell wall problems, it might improve things sufficiently to prevent effects on the T3SS and surface attachment. However, another possibility is that MepM plays a more specialized role. In this regard, it is intriguing to note that the assembly of transenvelope systems, including a T3SS, requires rearrangement of the peptidoglycan (42–44). Some T3SS-encoding loci encode a peptidoglycan hydrolase that is needed for T3SS function (45, 46). Unlike MepM, these are lytic transglycosylases, but it is still possible that a specific role of MepM is important for T3SS assembly or function in *P. aeruginosa*. Indeed, many T3SS loci do not encode a dedicated peptidoglycan hydrolase, raising the possibility that they rely on endogenous cellular hydrolase(s). It is also worth noting the possibility that some peptidoglycan hydrolases function in a complex and removing one of them destroys the function of the entire complex. The lytic transglycosylases MltD and RlpA were pulled down by the LbcA-CtpA-S302A trap, but they do not appear to be CtpA substrates (Fig. 4B and 8A). This could be explained by an interaction with a CtpA substrate such as MepM.

The MepM and PA4404 substrates are in the LytM/M23 family of peptidases, and both have homology to *E. coli* MepM. However, indirect genetic evidence suggests that Prc, the only CTP in *E. coli*, might not degrade MepM in that species (47). *E. coli* Prc does degrade the NlpC/P60 peptidase family member MepS (22). This is notable, because the CtpA substrates PA1198 and PA1199 are both homologous to *E. coli* MepS. Therefore, despite being from divergent CTP subfamilies, *P. aeruginosa* CtpA and *E. coli* Prc both degrade MepS-like hydrolases. This is surprising because *P. aeruginosa* has a second CTP, and the other one is a homologue of *E. coli* Prc (PA3257, also known as AlgO). The abundance of PA1198 and PA1199 in a $\Delta ctpA$ strain (Fig. 8A) suggests that Prc might not degrade MepS hydrolases in *P. aeruginosa*.

P. aeruginosa Prc was proposed to cleave the anti-sigma factor MucA, inducing the extracytoplasmic function (ECF) sigma factor AlgT/U and alginate production (26–28). However, the AlgT/U regulon can also be induced by cell wall-inhibitory antibiotics (28). Therefore, it is possible that *P. aeruginosa* Prc cleaves one or more peptidoglycan-modifying enzymes, and its impact on the AlgT/U regulon is a consequence of altered peptidoglycan rather than Prc cleaving MucA directly. In fact, CtpA overproduction induces an ECF sigma factor that can be activated by the cell wall-inhibitory antibiotic D-cycloserine, but CtpA is unlikely to cleave its anti-sigma factor (18). Prc has also been implicated in activating several other ECF sigma factors in *Pseudomonas* species (48). However, induction of ECF sigma factors by cell wall stress is common, and an effect of Prc on peptidoglycan could perhaps be the explanation. Importantly, Prc has not been shown to cleave any anti-sigma factor directly.

In summary, a binary protein complex degrades at least four proteins predicted to cleave peptidoglycan cross-links in *P. aeruginosa* (Fig. 9). Therefore, LbcA-CtpA might be an important mechanism used to control peptidoglycan hydrolysis, a reaction with the potential for catastrophic consequences if it is not carefully constrained. Importantly, similarities to the distantly related Nlpl-Prc system of *E. coli* suggest that this might be a widespread phenomenon in diverse bacteria.

MATERIALS AND METHODS

Bacterial strains and standard growth conditions. The strains and plasmids used in this study are listed in Table 1. Bacteria were grown routinely in Luria-Bertani (LB) broth or on LB agar at 37°C. During conjugation procedures, *P. aeruginosa* was occasionally selected on Vogel-Bonner minimal (VBM) agar. *E. coli* K-12 strain SM10 was used to conjugate plasmids into *P. aeruginosa* (49).

Plasmid and strain constructions. To construct in-frame deletion mutants, two fragments of ~0.5 kb each corresponding to regions upstream and downstream of the deletion site were amplified by PCR and cloned into pEX18Ap. The plasmids were integrated into the *P. aeruginosa* chromosome after conjugation from *E. coli*, and sucrose-resistant, carbenicillin-sensitive segregants were isolated on LB agar containing 10% sucrose. Deletions were verified by colony PCR. Δ *lbcA::aacC1* mutants were constructed similarly, except the *aacC1* cassette from plasmid p34s-Gm was cloned between the upstream and downstream fragments in pEX18Ap.

To make strain AJDP1140, encoding CtpA-S302A, 2 ~0.5-kb fragments flanking codon 302 of *ctpA* were amplified by PCR chromosome. For each fragment, one of the primers incorporated a mismatch at codon 302 to convert it to encode alanine. The fragments were joined in a PCR splicing by overlap extension (SOEing) reaction (50) via their overlapping regions around codon 302. The product was cloned into pEX18Ap and exchanged for the corresponding region of the *ctpA* gene by integration, selection for sucrose-resistant segregants, and confirmation by colony PCR and DNA sequencing.

To make strains encoding CtpA-FLAG-His₆ and CtpA-S302A-FLAG-His₆, 2 ~500-bp fragments surrounding the stop codon of *ctpA* were amplified by PCR. For each fragment, one primer incorporated a region encoding FLAG-His₆. The fragments were joined in a PCR SOEing reaction via their overlapping FLAG-His₆ sequences. The products were cloned into plasmid pEX18Ap and used to fuse the FLAG-His₆-encoding region to the *ctpA* gene by integration, selection for sucrose-resistant segregants, and confirmation by colony PCR and DNA sequencing.

Plasmids encoding C-terminal FLAG-tagged proteins were constructed by amplifying genes using a downstream primer that incorporated a region encoding the FLAG tag and then cloning into pHERD20T or pVLT35. Plasmids for protein overproduction and purification were constructed by PCR amplification of genes, without their predicted N-terminal signal sequences and stop codons, and cloning into pET-24b(+) to encode C-terminal His₆-tagged versions.

Polyclonal antiserum production and immunoblotting. *E. coli* strain ER2566 (NEB) containing a pET-24b(+) derivative encoding MepM-His₆, LbcA-His₆, or OprF-His₆ was grown in LB broth to the mid-log phase at 37°C with aeration. Protein production was induced with 1 mM IPTG (isopropyl-β-D-thiogalactopyranoside) for 4 h at 37°C for LbcA-His₆ and OprF-His₆ or overnight at 16°C for MepM-His₆. Proteins were purified under denaturing conditions by nickel-nitrilotriacetic acid (NTA) affinity chromatography as described by the manufacturer (Qiagen). Polyclonal rabbit antisera were raised by Covance Research Products, Inc.

Semidry electroblotting was used to transfer SDS-PAGE-separated samples to nitrocellulose. Chemiluminescent detection followed incubation with polyclonal antiserum or monoclonal antibody and then goat anti-rabbit IgG (Sigma) or goat anti-mouse IgG (Sigma)-horseradish peroxidase conjugates used at the manufacturer's recommended dilution. Primary antisera or antibodies were diluted 5,000-fold for anti-THE-His (GenScript) and anti-FLAG M2 (Sigma), 7,500-fold for anti-MepM, 8,000-fold for anti-LbcA, 10,000-fold for anti-PA0943, anti-PA4068, and anti-CtpA (18, 51), and 20,000-fold for anti-OprF.

CtpA-FLAG-His₆ tandem purification. Strains were grown in 100 ml LB broth at 37°C with aeration to an OD₆₀₀ of ~1.2 to 1.4, and cells were collected by centrifugation. For formaldehyde cross-linking, the pellet was washed with cold 10 mM potassium phosphate buffer (pH 8.0) and resuspended to an OD₆₀₀ of 5 in the same buffer. One percent formaldehyde was added, followed by incubation at room

TABLE 1 *P. aeruginosa* strains and plasmids used in this study

Strain or plasmid	Genotype	Reference or source
Strains		
PAK ^a	Wild type	52
AJDP566	<i>pscC::pAJD1</i>	18
AJDP730	Δ <i>ctpA</i>	18
AJDP1091	Δ <i>lbcA::aacC1</i>	This study
AJDP1133	Φ [<i>ctpA</i> -FLAG-His ₆]	This study
AJDP1140	<i>ctpA</i> -S302A	This study
AJDP1153	Φ [<i>ctpA</i> -S302A-FLAG-His ₆]	This study
AJDP1228	Δ <i>mepM</i>	This study
AJDP1229	Δ <i>ctpA</i> Δ <i>mepM</i>	This study
AJDP1230	Δ <i>lbcA::aacC1</i> Δ <i>mepM</i>	This study
Plasmids		
pHERD20T	Amp ^r pMB1 <i>ori araBp</i> expression vector	53
pET-24b(+)	Kan ^r pMB1 <i>ori</i> T7p expression vector	Novagen
pEX18Ap	Amp ^r pMB1 <i>ori oriT sacB</i> ⁺	54
pVLT35	Sm ^r Sp ^r RSF1010 <i>ori tacp</i> expression vector	55
p34s-Gm	Apr ^r <i>aacC1</i> ⁺ (Gm ^r) pUC <i>ori</i>	56
pAJD2290	T7p-' <i>ctpA</i> -His ₆ in pET-24b(+)	18
pAJD2003	T7p-' <i>oprF</i> -His ₆ in pET-24b(+)	This study
pAJD2350	<i>tacp-ctpA</i> -His ₆ in pVLT35	18
pAJD2351	<i>tacp-ctpA</i> -S302A-His ₆ in pVLT35	18
pAJD2226	<i>araBp-ctpA</i> -His ₆ in pHERD20T	18
pAJD2227	<i>araBp-ctpA</i> -S302A-His ₆ in pHERD20T	18
pAJD2443	<i>tacp-lbcA</i> -FLAG in pVLT35	This study
pAJD2653	T7p-' <i>lbcA</i> -His ₆ in pET-24b(+)	This study
pAJD2655	T7p-' <i>ctpA</i> -S302A-His ₆ in pET-24b(+)	This study
pAJD2779	<i>araBp-mepM</i> -FLAG in pHERD20T	This study
pAJD2801	<i>araBp-PA3623</i> -FLAG in pHERD20T	This study
pAJD2809	T7p-' <i>mepM</i> -His ₆ in pET-24b(+)	This study
pAJD2816	<i>araBp-PA1812</i> -FLAG in pHERD20T	This study
pAJD2817	<i>araBp-PA4404</i> -FLAG in pHERD20T	This study
pAJD2818	<i>araBp-PA3787</i> -FLAG in pHERD20T	This study
pAJD2820	<i>araBp-PA1198</i> -FLAG in pHERD20T	This study
pAJD2821	<i>araBp-PA1199</i> -FLAG in pHERD20T	This study
pAJD2832	T7p-' <i>PA1198</i> -His ₆ in pET-24b(+)	This study
pAJD2833	T7p-' <i>PA3787</i> -His ₆ in pET-24b(+)	This study
pAJD2834	T7p-' <i>PA4404</i> -His ₆ in pET-24b(+)	This study
pAJD2835	<i>araBp-PA0639</i> -FLAG in pHERD20T	This study
pAJD2836	<i>araBp-PA1844</i> -FLAG in pHERD20T	This study
pAJD2837	<i>araBp-PA2272</i> -FLAG in pHERD20T	This study
pAJD2839	<i>araBp-PA5363</i> -FLAG in pHERD20T	This study
pAJD2840	<i>araBp-PA5551</i> -FLAG in pHERD20T	This study
pAJD2842	<i>araBp-PA4418</i> -FLAG in pHERD20T	This study
pAJD2844	T7p-' <i>PA1199</i> -His ₆ in pET-24b(+)	This study
pAJD2877	<i>araBp-rlpA</i> -FLAG in pHERD20T	This study

^aAll *P. aeruginosa* strains shown are derivatives of strain PAK.

temperature for 30 min. A 0.3 M concentration of Tris-HCl (pH 7.5) was added to quench, and the cells were collected by centrifugation. Pellets were resuspended in 3 ml lysis buffer (50 mM Tris-HCl [pH 7.5], 150 mM NaCl, 5 mM imidazole), and Roche complete protease inhibitors (2 × concentration), 1 μg/ml DNase I, 1 μg/ml RNase, and 1 mg/ml lysozyme were added. Cells were disrupted by sonication, and then 1% *n*-dodecyl β-D-maltoside (DDM) was added followed by incubation with rotation for 30 min at 4°C. Insoluble material was removed by centrifugation at 13,000 × *g* for 30 min at 4°C. Two hundred microliters of nickel-NTA agarose in lysis buffer was added to the supernatant, followed by incubation with rotation for 1.5 h at 4°C. The resin was collected in a drip column and washed with 4 ml lysis buffer and then 4 ml lysis buffer containing 20 mM imidazole. Proteins were eluted in 1 ml lysis buffer containing 250 mM imidazole, mixed with 30 μl anti-FLAG M2 agarose resin (Sigma) in Tris-buffered saline (TBS: 10 mM Tris-HCl [pH 7.5], 150 mM NaCl), and incubated with rotation for 2 h at 4°C. A 1-ml spin column (Pierce 69725) was used to wash the resin three times with 800 μl TBS. Proteins were eluted by adding 100 μl of 200 μg/ml FLAG peptide (Sigma F3290) in TBS and incubating the mixture with rotation at 4°C for 30 min. Proteins were identified by liquid chromatography-mass spectrometry (LC-MS) (NYU School of Medicine Proteomics Laboratory).

CtpA-His₆, LbcA-FLAG tandem purification. Δ *ctpA* strains containing pVLT35 derivatives encoding CtpA-His₆ or CtpA-S302A-His₆ and pHERD20T encoding LbcA-FLAG were inoculated to an OD₆₀₀ of 0.05 in 250 ml LB broth containing 5 mM EGTA, 100 μM IPTG, and 0.02% (wt/vol) arabinose. Cultures were

incubated at 37°C with 225-rpm rotation until the OD₆₀₀ was ~1.5. Procedures described in the preceding section were used for protein purification and identification.

Analysis of T3SS substrates in cell-free supernatants. Strains were inoculated at an OD₆₀₀ of 0.04 in test tubes containing 5 ml tryptic soy broth (TSB) containing 5 mM EGTA and grown for 6 h at 37°C on a roller. Cells from the equivalent of 1 ml of culture at an OD₆₀₀ of 1.5 were removed by centrifugation at $3,300 \times g$ for 15 min at 4°C. The supernatant was filtered with a 0.22- μ m-pore filter, and then 1/10 volume trichloroacetic acid was added, followed by incubation at 4°C overnight. Proteins were collected by centrifugation at $4,500 \times g$ for 40 min at 4°C, washed twice with 1 ml ice-cold acetone, dried at room temperature for 30 to 40 min, and resuspended in SDS-PAGE sample buffer. Proteins were separated by SDS-PAGE and stained with silver.

Surface attachment. Saturated cultures in LB broth were diluted to an OD₆₀₀ of 0.1 in 13- by 100-mm borosilicate glass tubes containing 0.5 ml of M63 salts supplemented with 1 mM MgSO₄, 0.5% (wt/vol) Casamino Acids, and 0.2% (wt/vol) glucose. The tubes were incubated at 30°C without agitation for 8 h. Culture medium was removed, and the tubes were washed twice with 2 ml of water. Five hundred microliters of 0.1% (wt/vol) crystal violet was added, followed by incubation at room temperature for 10 min and two washes with 10 ml water, and then the tubes were inverted for 10 min at room temperature and photographed. The crystal violet was dissolved in 1 ml ethanol, and absorbance at 595 nm was measured. A tube that contained growth medium alone was used to generate the blank.

Subcellular fractionation. Osmotic shock was done as described previously (18), except that cultures were grown to an OD₆₀₀ of ~1. To generate soluble and insoluble fractions, 100-ml cultures in LB broth were grown at 37°C with shaking at 225 rpm to an OD₆₀₀ of ~1. Cells were collected by centrifugation, washed with 10 ml of 20 mM Tris-HCl (pH 7.5)–20 mM EDTA (TE), resuspended in 10 ml cold TE containing Roche complete protease inhibitors, and lysed by two passages through a French pressure cell (1,100 lb/in²). Intact cells were removed by centrifugation at $8,000 \times g$ for 10 min at 4°C. The supernatant was centrifuged at $100,000 \times g$ for 1 h at 4°C. The supernatant was the soluble fraction. The pellet (membrane fraction) was washed twice with 20 mM Tris-HCl (pH 7.5) and resuspended in 20 mM Tris-HCl (pH 7.5) containing Roche complete protease inhibitors.

CHO-K1 cell cytotoxicity. Chinese hamster ovary cells were grown in RPMI 1640 medium with 10% fetal bovine serum (FBS) and 2 mM glutamine at 37°C in a 5% CO₂ atmosphere. A total of 2×10^5 cells/well were seeded in a 24-well plate and incubated at 37°C for 16 h. Attached cells were washed with phosphate-buffered saline (PBS) and covered with RPMI 1640 containing 1% FBS and 2 mM glutamine. *P. aeruginosa* cells were grown in TSB at 37°C until the OD₆₀₀ was 0.8 and then added to the CHO-K1 cells at a multiplicity of infection of ~10. The plate was centrifuged at $250 \times g$ for 5 min and incubated for 4 h at 37°C. Supernatants were collected after centrifugation at $250 \times g$ for 5 min, and the lactate dehydrogenase (LDH) concentration was measured with the LDH Cytotox assay (Promega).

Cell wall isolation and digestion. Bacteria were grown to saturation in 500 ml LB broth at 37°C with 150-rpm shaking. Cells were harvested by centrifugation at $5,200 \times g$ for 20 min, resuspended in PBS, and sterilized by boiling for 60 min. Samples were bead beaten (Bead Mill 24; Fisher Scientific) with 0.5-mm-diameter glass beads for 10 1-min cycles with 1-min rests. Beads were removed using a Steriflip 20- μ m-pore nylon vacuum filter (EMD Millipore). Crude cell wall pellets were resuspended in 2 ml PBS, to which 8 ml of 2% SDS (wt/vol) was added. They were boiled for 60 min, washed with deionized water, and resuspended in 2 ml of 50 mM Tris (pH 8.0). DNase (200 μ g) was added, and the mixture was incubated at 37°C for 24 h and 150 rpm, followed by 200 μ g pronase E and another 24 h of incubation. Cell walls were washed once, resuspended in 1 ml of 50 mM Tris (pH 8.0), and then digested by adding 500 units of mutanolysin (Sigma-Aldrich) and incubating the mixture at room temperature for 24 h. Another 500 units of mutanolysin was added, followed by another 24-h incubation. Digested cell walls were frozen, lyophilized, and dissolved in 1 ml of 0.375 M sodium borate buffer (pH 9.0) using high-performance liquid chromatography (HPLC)-grade water. Muropeptides were reduced by adding 10 mg of sodium borohydride at room temperature for 30 min. Reduction was quenched by adding 125 μ l phosphoric acid. Samples were frozen at –80°C, lyophilized, resuspended in 1 ml of 1% trifluoroacetic acid, centrifuge filtered, and cleaned up for liquid chromatography-mass spectrometry (LC-MS) using 100- μ l Pierce C₁₈ tips.

Peptidoglycan analysis by liquid chromatography-mass spectrometry. Mutanolysin-digested muropeptide fragments were separated using a NanoACQUITY Ultra performance liquid chromatography system (Waters). A reverse-phase BEH C₁₈ column (length, 100 mm; diameter, 75 μ m) of 1.7- μ m beads with a pore size of 130 Å was used. Separation was carried out by injecting 2 μ l of mutanolysin-digested peptidoglycan from a 5- μ l sample loop into the column under an isocratic condition of 98% mobile phase A (0.1% formic acid in HPLC water) and 2% mobile phase B (90% acetonitrile and 10% of HPLC water added with 0.1% formic acid) for 5 min, and then a linear gradient to 50% buffer B was applied for 30 min. The column was regenerated under the isocratic condition with 85% buffer B for 5 min, a linear gradient to 98% buffer A for 1 min, and then isocratic at 98% buffer A for 23 min. The flow rate was kept constant (0.6 μ l/min) throughout the analysis. Fibrinopeptide B (Glu-Fib) was used as an internal standard. Data were analyzed using MassLynx (Waters) and MatLab (MathWorks, Inc.).

In vitro proteolysis. *E. coli* ER2566 cells (NEB) containing each pET-24b(+) derivative were grown in 1 liter of LB broth at 37°C with aeration until the OD₆₀₀ was 0.6 to 0.8. Protein production was induced by adding 1 mM IPTG and incubating the mixture for 16 h at 16°C with aeration. Proteins were purified under native conditions by NTA agarose affinity chromatography as recommended by the manufacturer (Qiagen). Following elution with imidazole, proteins were exchanged into 50 mM NaH₂PO₄–300 mM NaCl (pH 8.0), using Amicon Ultra-4 centrifuge filter devices (10-kDa cutoff), and then supplemented with 10% glycerol and stored at –20°C. However, CtpA-His₆ and CtpA-S302A-His₆ only were eluted sequentially

with 50 mM NaH₂PO₄–300 mM NaCl (pH 8.0), containing 50, 100, 150, 200, or 250 mM imidazole. Buffer exchange and freezing were not possible due to precipitation. Therefore, CtpA-His₆ and CtpA-S302A-His₆ were purified, stored at 4°C, and used within 48 h. All experiments were done at least three times, with representative experiments shown in the figures.

Growth curves. Saturated cultures were diluted into 5 ml of LB broth, containing either 1% (wt/vol) NaCl or no NaCl, in 18-mm-diameter test tubes so that the initial OD₆₀₀ was approximately 0.04. The cultures were grown on a roller drum at 37°C for 9 h, and 0.1-ml samples were removed at hourly intervals for OD₆₀₀ measurement.

SUPPLEMENTAL MATERIAL

Supplemental material for this article may be found at <https://doi.org/10.1128/mBio.00972-18>.

FIG S1, PDF file, 0.5 MB.

TABLE S1, PDF file, 0.1 MB.

ACKNOWLEDGMENTS

Research was supported by an Investigators in Pathogenesis of Infectious Disease Award from the Burroughs Wellcome Fund to A.J.D., and by the National Institute of Allergy and Infectious Diseases (NIAID) of the National Institutes of Health, under award no. R21AI117131 and R01AI136901. Mass spectrometric protein identification done by the NYU School of Medicine Proteomics Laboratory was partly supported by the NYU School of Medicine. S.J.K. and B.R., who conducted the peptidoglycan analysis and analyzed the data, were supported by National Institutes of Health grant GM116130 and acknowledge the Baylor University Mass Spectrometry Centre (BU-MS) for support. The content is solely the responsibility of the authors and does not necessarily represent the official views of the National Institutes of Health.

We thank Sindhoora Singh for constructing plasmid pAJD2003.

REFERENCES

- Driscoll JA, Brody SL, Kollef MH. 2007. The epidemiology, pathogenesis and treatment of *Pseudomonas aeruginosa* infections. *Drugs* 67:351–368. <https://doi.org/10.2165/00003495-200767030-00003>.
- Hauser AR. 2009. The type III secretion system of *Pseudomonas aeruginosa*: infection by injection. *Nat Rev Microbiol* 7:654–665. <https://doi.org/10.1038/nrmicro2199>.
- Wagner VE, Iglewski BH. 2008. *P. aeruginosa* biofilms in CF infection. *Clin Rev Allergy Immunol* 35:124–134. <https://doi.org/10.1007/s12016-008-8079-9>.
- Clark ST, Diaz Caballero J, Cheang M, Coburn B, Wang PW, Donaldson SL, Zhang Y, Liu M, Keshavjee S, Yau YCW, Waters VJ, Elizabeth Tullis D, Guttman DS, Hwang DM. 2015. Phenotypic diversity within a *Pseudomonas aeruginosa* population infecting an adult with cystic fibrosis. *Sci Rep* 5:10932. <https://doi.org/10.1038/srep10932>.
- Moore NM, Flaws ML. 2011. Epidemiology and pathogenesis of *Pseudomonas aeruginosa* infections. *Clin Lab Sci* 24:43–46.
- Lyczak JB, Cannon CL, Pier GB. 2000. Establishment of *Pseudomonas aeruginosa* infection: lessons from a versatile opportunist. *Microbes Infect* 2:1051–1060. [https://doi.org/10.1016/S1286-4579\(00\)01259-4](https://doi.org/10.1016/S1286-4579(00)01259-4).
- Rawlings ND, Barrett AJ, Bateman A. 2010. Merops: the peptidase database. *Nucleic Acids Res* 38:D227–D233. <https://doi.org/10.1093/nar/gkp971>.
- Hara H, Yamamoto Y, Higashitani A, Suzuki H, Nishimura Y. 1991. Cloning, mapping, and characterization of the *Escherichia coli* *prc* gene, which is involved in C-terminal processing of penicillin-binding protein 3. *J Bacteriol* 173:4799–4813. <https://doi.org/10.1128/jb.173.15.4799-4813.1991>.
- Keiler KC, Silber KR, Downard KM, Papayannopoulos IA, Biemann K, Sauer RT. 1995. C-terminal specific protein degradation: activity and substrate specificity of the Tsp protease. *Protein Sci* 4:1507–1515. <https://doi.org/10.1002/pro.5560040808>.
- Che Y, Fu A, Hou X, McDonald K, Buchanan BB, Huang W, Luan S. 2013. C-terminal processing of reaction center protein D1 is essential for the function and assembly of photosystem II in *Arabidopsis*. *Proc Natl Acad Sci U S A* 110:16247–16252. <https://doi.org/10.1073/pnas.1313894110>.
- Satoh K, Yamamoto Y. 2007. The carboxyl-terminal processing of precursor D1 protein of the photosystem II reaction center. *Photosynth Res* 94:203–215. <https://doi.org/10.1007/s11120-007-9191-z>.
- Kumru OS, Bunikis I, Sorokina I, Bergström S, Zückert WR. 2011. Specificity and role of the *Borrelia burgdorferi* CtpA protease in outer membrane protein processing. *J Bacteriol* 193:5759–5765. <https://doi.org/10.1128/JB.05622-11>.
- Bandara AB, DeShazer D, Inzana TJ, Sriranganathan N, Schurig GG, Boyle SM. 2008. A disruption of *ctpA* encoding carboxy-terminal protease attenuates *Burkholderia mallei* and induces partial protection in CD1 mice. *Microb Pathog* 45:207–216. <https://doi.org/10.1016/j.micpath.2008.05.005>.
- Bandara AB, Sriranganathan N, Schurig GG, Boyle SM. 2005. Carboxyl-terminal protease regulates *Brucella suis* morphology in culture and persistence in macrophages and mice. *J Bacteriol* 187:5767–5775. <https://doi.org/10.1128/JB.187.16.5767-5775.2005>.
- Carroll RK, Rivera FE, Cavaco CK, Johnson GM, Martin D, Shaw LN. 2014. The lone S41 family C-terminal processing protease in *Staphylococcus aureus* is localized to the cell wall and contributes to virulence. *Microbiology* 160:1737–1748. <https://doi.org/10.1099/mic.0.079798-0>.
- Deng CY, Deng AH, Sun ST, Wang L, Wu J, Wu Y, Chen XY, Fang RX, Wen TY, Qian W. 2014. The periplasmic PDZ domain-containing protein Prc modulates full virulence, envelopes stress responses, and directly interacts with dipeptidyl peptidase of *Xanthomonas oryzae* pv. *oryzae*. *Mol Plant Microbe Interact* 27:101–112. <https://doi.org/10.1094/MPMI-08-13-0234-R>.
- Mitchell SJ, Minnick MF. 1997. A carboxy-terminal processing protease gene is located immediately upstream of the invasion-associated locus from *Bartonella bacilliformis*. *Microbiology* 143:1221–1233. <https://doi.org/10.1099/00221287-143-4-1221>.
- Seo J, Darwin AJ. 2013. The *Pseudomonas aeruginosa* periplasmic protease CtpA can affect systems that impact its ability to mount both acute and chronic infections. *Infect Immun* 81:4561–4570. <https://doi.org/10.1128/IAI.01035-13>.
- Lad SP, Yang G, Scott DA, Wang G, Nair P, Mathison J, Reddy VS, Li E. 2007. Chlamydial CT441 is a PDZ domain-containing tail-specific protease that interferes with the NF-kappaB pathway of immune response. *J Bacteriol* 189:6619–6625. <https://doi.org/10.1128/JB.00429-07>.
- Seoane A, Sabbaj A, McMurry LM, Levy SB. 1992. Multiple antibiotic

- susceptibility associated with inactivation of the *prc* gene. *J Bacteriol* 174:7844–7847. <https://doi.org/10.1128/jb.174.23.7844-7847.1992>.
21. Wang CY, Wang SW, Huang WC, Kim KS, Chang NS, Wang YH, Wu MH, Teng CH. 2012. Prc contributes to *Escherichia coli* evasion of classical complement-mediated serum killing. *Infect Immun* 80:3399–3409. <https://doi.org/10.1128/IAI.00321-12>.
 22. Singh SK, Parveen S, SaiSree L, Reddy M. 2015. Regulated proteolysis of a cross-link-specific peptidoglycan hydrolase contributes to bacterial morphogenesis. *Proc Natl Acad Sci U S A* 112:10956–10961. <https://doi.org/10.1073/pnas.1507760112>.
 23. Singh SK, SaiSree L, Amrutha RN, Reddy M. 2012. Three redundant murein endopeptidases catalyze an essential cleavage step in peptidoglycan synthesis of *Escherichia coli* K12. *Mol Microbiol* 86:1036–1051. <https://doi.org/10.1111/mmi.12058>.
 24. Silber KR, Keiler KC, Sauer RT. 1992. Tsp: a tail-specific protease that selectively degrades proteins with nonpolar C termini. *Proc Natl Acad Sci U S A* 89:295–299. <https://doi.org/10.1073/pnas.89.1.295>.
 25. Keiler KC, Waller PR, Sauer RT. 1996. Role of a peptide tagging system in degradation of proteins synthesized from damaged messenger RNA. *Science* 271:990–993. <https://doi.org/10.1126/science.271.5251.990>.
 26. Reiling SA, Jansen JA, Henley BJ, Singh S, Chattin C, Chandler M, Rowen DW. 2005. Prc protease promotes mucoidy in *mutA* mutants of *Pseudomonas aeruginosa*. *Microbiology* 151:2251–2261. <https://doi.org/10.1099/mic.0.27772-0>.
 27. Sautter R, Ramos D, Schnepel L, Ciofu O, Wassermann T, Koh CL, Heydorn A, Hentzer M, Høiby N, Kharazmi A, Molin S, Devries CA, Ohman DE, Mathee K. 2012. A complex multilevel attack on *Pseudomonas aeruginosa* *algT/U* expression and *algT/U* activity results in the loss of alginate production. *Gene* 498:242–253. <https://doi.org/10.1016/j.gene.2011.11.005>.
 28. Wood LF, Leech AJ, Ohman DE. 2006. Cell wall-inhibitory antibiotics activate the alginate biosynthesis operon in *Pseudomonas aeruginosa*: roles of σ^{22} (AlgT) and the AlgW and Prc proteases. *Mol Microbiol* 62:412–426. <https://doi.org/10.1111/j.1365-2958.2006.05390.x>.
 29. Hoge R, Laschinski M, Jaeger KE, Wilhelm S, Rosenau F. 2011. The subcellular localization of a C-terminal processing protease in *Pseudomonas aeruginosa*. *FEMS Microbiol Lett* 316:23–30. <https://doi.org/10.1111/j.1574-6968.2010.02181.x>.
 30. Yeung AT, Torfs EC, Jamshidi F, Bains M, Wiegand I, Hancock RE, Overhage J. 2009. Swarming of *Pseudomonas aeruginosa* is controlled by a broad spectrum of transcriptional regulators, including MetR. *J Bacteriol* 191:5592–5602. <https://doi.org/10.1128/JB.00157-09>.
 31. Blatch GL, Lässle M. 1999. The tetratricopeptide repeat: a structural motif mediating protein-protein interactions. *Bioessays* 21:932–939. [https://doi.org/10.1002/\(SICI\)1521-1878\(199911\)21:11<932::AID-BIES5>3.0.CO;2-N](https://doi.org/10.1002/(SICI)1521-1878(199911)21:11<932::AID-BIES5>3.0.CO;2-N).
 32. Wurtzel O, Yoder-Himes DR, Han K, Dandekar AA, Edelheit S, Greenberg EP, Sorek R, Lory S. 2012. The single-nucleotide resolution transcriptome of *Pseudomonas aeruginosa* grown in body temperature. *PLoS Pathog* 8:e1002945. <https://doi.org/10.1371/journal.ppat.1002945>.
 33. O'Toole GA, Kolter R. 1998. Initiation of biofilm formation in *Pseudomonas fluorescens* WCS365 proceeds via multiple, convergent signalling pathways: a genetic analysis. *Mol Microbiol* 28:449–461. <https://doi.org/10.1046/j.1365-2958.1998.00797.x>.
 34. Lee VT, Smith RS, Tümmler B, Lory S. 2005. Activities of *Pseudomonas aeruginosa* effectors secreted by the type III secretion system in vitro and during infection. *Infect Immun* 73:1695–1705. <https://doi.org/10.1128/IAI.73.3.1695-1705.2005>.
 35. Chang JD, Foster EE, Thadani AN, Ramirez AJ, Kim SJ. 2017. Inhibition of *Staphylococcus aureus* cell wall biosynthesis by desleucyl-oritavancin: a quantitative peptidoglycan composition analysis by mass spectrometry. *J Bacteriol* 199:e00278-17. <https://doi.org/10.1128/JB.00278-17>.
 36. Chang JD, Foster EE, Wallace AG, Kim SJ. 2017. Peptidoglycan O-acetylation increases in response to vancomycin treatment in vancomycin-resistant *Enterococcus faecalis*. *Sci Rep* 7:46500. <https://doi.org/10.1038/srep46500>.
 37. Chang JD, Foster EE, Yang H, Kim SJ. 2017. Quantification of the D-Ala-D-Lac-terminated peptidoglycan structure in vancomycin-resistant *Enterococcus faecalis* using a combined solid-state nuclear magnetic resonance and mass spectrometry analysis. *Biochemistry* 56:612–622. <https://doi.org/10.1021/acs.biochem.6b00774>.
 38. Bateman A, Bycroft M. 2000. The structure of a LysM domain from *E. coli* membrane-bound lytic murein transglycosylase D (MltD). *J Mol Biol* 299:1113–1119. <https://doi.org/10.1006/jmbi.2000.3778>.
 39. Lee M, Heseck D, Llarrull LI, Lastochkin E, Pi H, Boggess B, Mobashery S. 2013. Reactions of all *Escherichia coli* lytic transglycosylases with bacterial cell wall. *J Am Chem Soc* 135:3311–3314. <https://doi.org/10.1021/ja309036q>.
 40. Jorgenson MA, Chen Y, Yahashiri A, Popham DL, Weiss DS. 2014. The bacterial septal ring protein RlpA is a lytic transglycosylase that contributes to rod shape and daughter cell separation in *Pseudomonas aeruginosa*. *Mol Microbiol* 93:113–128. <https://doi.org/10.1111/mmi.12643>.
 41. Su MY, Som N, Wu CY, Su SC, Kuo YT, Ke LC, Ho MR, Tzeng SR, Teng CH, Mengin-Lecreux D, Reddy M, Chang CI. 2017. Structural basis of adaptor-mediated protein degradation by the tail-specific PDZ-protease Prc. *Nat Commun* 8:1516. <https://doi.org/10.1038/s41467-017-01697-9>.
 42. Dijkstra AJ, Keck W. 1996. Peptidoglycan as a barrier to transenvelope transport. *J Bacteriol* 178:5555–5562. <https://doi.org/10.1128/jb.178.19.5555-5562.1996>.
 43. Koraimann G. 2003. Lytic transglycosylases in macromolecular transport systems of Gram-negative bacteria. *Cell Mol Life Sci* 60:2371–2388. <https://doi.org/10.1007/s00018-003-3056-1>.
 44. Scheurwater EM, Burrows LL. 2011. Maintaining network security: how macromolecular structures cross the peptidoglycan layer. *FEMS Microbiol Lett* 318:1–9. <https://doi.org/10.1111/j.1574-6968.2011.02228.x>.
 45. Burkinshaw BJ, Deng W, Lameignère E, Wasney GA, Zhu H, Worrall LJ, Finlay BB, Strynadka NC. 2015. Structural analysis of a specialized type III secretion system peptidoglycan-cleaving enzyme. *J Biol Chem* 290:10406–10417. <https://doi.org/10.1074/jbc.M115.639013>.
 46. Hausner J, Hartmann N, Jordan M, Büttner D. 2017. The predicted lytic transglycosylase HpaH from *Xanthomonas campestris* pv. vesicatoria associates with the type III secretion system and promotes effector protein translocation. *Infect Immun* 85:e00788-16. <https://doi.org/10.1128/IAI.00788-16>.
 47. Lai GC, Cho H, Bernhardt TG. 2017. The mecillinam resistome reveals a role for peptidoglycan endopeptidases in stimulating cell wall synthesis in *Escherichia coli*. *PLoS Genet* 13:e1006934. <https://doi.org/10.1371/journal.pgen.1006934>.
 48. Bastiaansen KC, Ibañez A, Ramos JL, Bitter W, Llamas MA. 2014. The Prc and RseP proteases control bacterial cell-surface signalling activity. *Environ Microbiol* 16:2433–2443. <https://doi.org/10.1111/1462-2920.12371>.
 49. Miller VL, Mekalanos JJ. 1988. A novel suicide vector and its use in construction of insertion mutations: osmoregulation of outer membrane proteins and virulence determinants in *Vibrio cholerae* requires *toxR*. *J Bacteriol* 170:2575–2583. <https://doi.org/10.1128/jb.170.6.2575-2583.1988>.
 50. Heckman KL, Pease LR. 2007. Gene splicing and mutagenesis by PCR-driven overlap extension. *Nat Protoc* 2:924–932. <https://doi.org/10.1038/nprot.2007.132>.
 51. Seo J, Brencic A, Darwin AJ. 2009. Analysis of secretin-induced stress in *Pseudomonas aeruginosa* suggests prevention rather than response and identifies a novel protein involved in secretin function. *J Bacteriol* 191:898–908. <https://doi.org/10.1128/JB.01443-08>.
 52. Strom MS, Lory S. 1986. Cloning and expression of the pilin gene of *Pseudomonas aeruginosa* PAK in *Escherichia coli*. *J Bacteriol* 165:367–372. <https://doi.org/10.1128/jb.165.2.367-372.1986>.
 53. Qiu D, Damron FH, Mima T, Schweizer HP, Yu HD. 2008. PBAD-based shuttle vectors for functional analysis of toxic and highly regulated genes in *Pseudomonas* and *Burkholderia* spp. and other bacteria. *Appl Environ Microbiol* 74:7422–7426. <https://doi.org/10.1128/AEM.01369-08>.
 54. Hoang TT, Karkhoff-Schweizer RR, Kutchna AJ, Schweizer HP. 1998. A broad-host-range Flp-FRT recombination system for site-specific excision of chromosomally-located DNA sequences: application for isolation of unmarked *Pseudomonas aeruginosa* mutants. *Gene* 212:77–86. [https://doi.org/10.1016/S0378-1119\(98\)00130-9](https://doi.org/10.1016/S0378-1119(98)00130-9).
 55. de Lorenzo V, Eltis L, Kessler B, Timmis KN. 1993. Analysis of *Pseudomonas* gene products using *lacI^q/P_{trp}-lac* plasmids and transposons that confer conditional phenotypes. *Gene* 123:17–24. [https://doi.org/10.1016/0378-1119\(93\)90533-9](https://doi.org/10.1016/0378-1119(93)90533-9).
 56. Dennis JJ, Zylstra GJ. 1998. Plasmids: modular self-cloning minitransposon derivatives for rapid genetic analysis of Gram-negative bacterial genomes. *Appl Environ Microbiol* 64:2710–2715.